Inorg. Chem. **2006**, *45*, 7593–7599

Inorganic Chemistry

Article

New Members in the $Ni_{n+1}(QO_3)_nX_2$ Family: Unusual 3D Network Based on Ni_4ClO_3 Cubane-like Clusters in $Ni_7(TeO_3)_6Cl_2$

Hai-Long Jiang and Jiang-Gao Mao*

State Key Laboratory of Structural Chemistry, Fujian Institute of Research on the Structure of Matter, and the Graduate School of the Chinese Academy of Sciences, Chinese Academy of Sciences, Fuzhou 350002, P. R. China

Received March 3, 2006

Three new members in the family of nickel(II) tellurium(IV)/selenium(IV) oxyhalides generally formulated as $Ni_{n+1}(QO_3)_nX_2$ (Q = Te, X = Cl, $n = 6$, 10; Q = Se, X = Br, $n = 4$) have been synthesized by solid-state reactions of NiX_2, QO_2, and NiO (or Ni_2O_3) at high temperature. The structure of $Ni_7(TeO_3)_6Cl_2$ features a novel 3D network based on Ni_4ClO_3 cubane-like clusters with Te atoms located at the cavities of the network. Ni_4ClO_3 clusters are interconnected into a hexagonal layer through additional O···O edges. The neighboring two layers are further interconnected, via sharing of common Ni(II) atoms, into a novel 3D network. The 3D open framework of $Ni_5(SeO_3)_4Br_2$ is built from 2D nickel(II) oxybromide layers bridged by Se and additional Ni atoms. The structure of $Ni_{11}(TeO_3)_{10}Cl_2$ features a condensed 3D network based on NiO_5Cl, NiO_6, and NiO_5 polyhedra interconnected via corner and edge sharing, as well as O–Te–O bridges. The results of magnetic property measurements indicate that all three compounds display antiferromagnetic interactions between nickel(II) centers.

Introduction

Selenites or tellurites can adopt many unusual structures because of the presence of the stereochemically active lone-pair electrons.[1] The asymmetric coordination polyhedron adopted by the Se(IV) or Te(IV) atom may result in noncentrosymmetric structures with consequent interesting physical properties, such as nonlinear optical second harmonic generation (SHG).[2−4] Transition metal ions with d^0 electronic configurations, such as Ti^{4+}, Nb^{5+}, W^{6+}, Mo^{6+}, etc, which are susceptible to second-order Jahn−Teller distortions have been introduced to the selenite or tellurite systems to enhance their SHG properties.[2−4] Recent studies also indicate that the activation of the selenite or tellurite anion for lanthanide ions can also produce new luminescent materials in the near-IR region.[5] More interestingly, transition metal Te(IV) or Se(IV) oxyhalides can be regarded as "chemical scissors", and some of them are promising new low-dimensional magnets.[6−9] A few compounds in the Cu system, such as $Cu_2Te_2O_5X_2$ (X = Cl, Br), $Cu_3(TeO_3)_2Br_2$, $Cu_3(SeO_3)_2Cl_2$, $Cu_5O_2(SeO_3)_2$, and $Cu_9O_2(SeO_3)_4Cl_6$, have been structurally characterized.[7,10−11] The corresponding

---

* To whom correspondence should be addressed. E-mail: mjg@ms.fjirsm.ac.cn.

(1) (a) Wickleder, M. S. *Chem. Rev.* **2002**, *102*, 2011 and references therein. (b) Harrison, W. T. A.; Dussack, L. L.; Jacobson, A. J. *Inorg. Chem.* **1994**, *33*, 6043. (c) Johnston, M. G.; Harrison, W. T. A. *J. Am. Chem. Soc.* **2002**, *124*, 4576. (d) Irvine, J. T. S.; Johnston, M. G.; Harrison, W. T. A. *Dalton Trans.* **2003**, 2641. (e) Almond, P. M.; Albrecht-Schmitt, T. E. *Inorg. Chem.* **2002**, *41*, 5495. (f) Almond, P. M.; Mckee, M. L.; Albrecht-Schmitt, T. E. *Angew. Chem., Int. Ed.* **2002**, *41*, 3426. (g) Harrison, W. T. A.; Phillips, M. L. F.; Stanchfield, J.; Nenoff, T. M. *Angew. Chem., Int. Ed.* **2000**, *39*, 3808. (h) Choudhury, A.; Kumar, U.; Rao, C. N. R. *Angew. Chem., Int. Ed.* **2002**, *41*, 158.

(2) (a) Ra, H.-S.; Ok, K.-M.; Halasyamani, S. H. *J. Am. Chem. Soc.* **2003**, *125*, 7764. (b) Ok, K.-M.; Halasyamani, P. S. *Inorg. Chem.* **2004**, *43*, 4248.

(3) (a) Hart, R. T.; Ok, K.-M.; Halasyamani, P. S.; Zwanziger, J. W. *Appl. Phys. Lett.* **2004**, *85*, 938. (b) Goodey, J.; Broussard, J.; Halasyamani, P. S. *Chem. Mater.* **2002**, *14*, 3174.

(4) (a) Johnston, M. G.; Harrison, W. T. A. *Inorg. Chem.* **2001**, *40*, 6518. (b) Balraj, V.; Vidyasagar, K. *Inorg. Chem.* **1999**, *38*, 5809.

(5) (a) Shen, Y.-L.; Jiang, H.-L.; Xu, J.; Mao, J.-G.; Cheah, K.-W. *Inorg. Chem.* **2005**, *44*, 9314. (b) Shen, Y.-L.; Mao, J.-G. *Inorg. Chem.* **2005**, *44*, 5328.

(6) Becker, R.; Johnsson, M.; Kremer, R.; Lemmens P. *Solid State Sci.* **2003**, *5*, 1411.

(7) Johnsson, M.; Törnroos, K. W.; Mila, F.; Millet, P. *Chem. Mater.* **2000**, *12*, 2853.

(8) Millet, P.; Bastide, B.; Pashchenko, V.; Gnatchenko, S.; Gapon, V.; Ksari, Y.; Stepanov, A. *J. Mater. Chem.* **2001**, *11*, 1152.

(9) Johnsson, M.; Törnroos, K. W.; Lemmens, P.; Millet, P. *Chem. Mater.* **2003**, *15*, 68.

(10) (a) Becker, R.; Johnsson, M.; Kremer, R.; Lemmens, P. *J. Solid State Chem.* **2005**, *178*, 2024. (b) Millet, P.; Bastide, B.; Johnsson, M. *Solid State Commun.* **2000**, *113*, 719.

(11) (a) Galy, J.; Bonnet, J. J.; Andersson, S. *Acta Chem. Scand.* **1979**, *A33*, 383. (b) Bastide, B.; Millet, P.; Johnsson, M.; Galy, J. *Mater. Res. Bull.* **2000**, *35*, 847.

10.1021/ic060356x CCC: $33.50

nickel system is much less explored, and only $Ni_5(TeO_3)_4X_2$ (X = Cl, Br), $Ni_5(SeO_3)_4Cl_2$, and three other nonstoichiometric compounds with approximate compositions of $[Ni_{30}Te_{32}O_{90}X_3][Ni_4X_{13}]$ (X = Cl, Br) have been reported.[9,12] We were astonished that many compounds in above systems can be generally formulated to be $M_{n+1}(QO_3)_nX_2$ where M, Q, and X represent a transition metal, Se or Te, and a halide anion, respectively. Our exploration of the missing members in the nickel system afforded three new compounds, namely, $Ni_{n+1}(QO_3)_nX_2$ (Q = Te, X = Cl, n = 6, 10; Q = Se, X = Br, n = 4). Herein, we report their syntheses, crystal structures, and magnetic properties.

Experimental Section

Materials and Instrumentation. All chemicals except NiO were analytically pure from commercial sources and used without further purification. Transition metal oxides and halides were purchased from the Shanghai Reagent Factory, and TeO_2 (99+%) and SeO_2 (99+%) were purchased from ACROS Organics. NiO was synthesized by heating Ni_2O_3 in air at 610 °C for 12 h, and its purity was confirmed by X-ray powder diffraction (XRD) studies. The measured XRD pattern is in good agreement with the one simulated from crystal structure data.[13] XRD patterns were collected on a XPERT-MPD $\theta-2\theta$ diffractometer. The chemical compositions for the three compounds were analyzed by a field-emission scanning electron microscope (FESEM, JSM6700F) equipped with an energy-dispersive X-ray spectroscope (EDS, Oxford INCA). IR spectra were recorded on a Magna 750 FT-IR spectrometer as KBr pellets in the range of 4000−400 cm^{-1}. Thermogravimetric analyses (TGA) were carried out with a NETZSCH STA 449C unit at a heating rate of 10 °C/min under an oxygen atmosphere. Magnetic susceptibility measurements were performed on a PPMS-9T magnetometer in the temperature range of 2−300 K.

Preparation of $Ni_7(TeO_3)_6Cl_2$ and $Ni_{11}(TeO_3)_{10}Cl_2$. Single crystals of both compounds were prepared by the solid-state reaction of a mixture of NiO (0.179 g, 2.4 mmol), $NiCl_2$ (0.078 g, 0.6 mmol), and TeO_2 (0.287 g, 1.8 mmol). The reaction mixture was thoroughly ground and pressed into a pellet, which was then sealed into an evacuated quartz tube. The quartz tube was heated at 710 °C for 6 days and then cooled to 310 °C at 4 °C/hr before the furnace was switched off. The products are $Ni_7(TeO_3)_6Cl_2$ (green, brick) as major phase, $Ni_{11}(TeO_3)_{10}Cl_2$ (brick, deep red), and previously reported $Ni_5(TeO_3)_4Cl_2$ (plate, orange), as two impurity phases.[9] Microprobe elemental analyses gave Ni/Te/Cl molar ratios of 7.0:6.0:2.3 and 11.2:9.8:2.4 for $Ni_7(TeO_3)_6Cl_2$ and $Ni_{11}(TeO_3)_{10}Cl_2$, respectively, which are in good agreement with those determined from single-crystal X-ray diffraction studies. A lot of effort was exerted to prepare single-phase products for $Ni_7(TeO_3)_6Cl_2$ and $Ni_{11}(TeO_3)_{10}Cl_2$ by the solid-state reactions of corresponding stoichiometric mixtures of NiO, $NiCl_2$, and TeO_2 at different temperatures. A pure powder sample of $Ni_{11}(TeO_3)_{10}Cl_2$ was obtained quantitatively by the reaction of a mixture of NiO/$NiCl_2$/TeO_2 in a molar ratio of 6:1:6 at 760 °C for 6 days. For $Ni_7(TeO_3)_6Cl_2$, the highest purity of about 90% was obtained by the reaction of a mixture of Ni_2O_3/$NiCl_2$/TeO_2 in a molar ratio of 3:1:6 at 620 °C for 6 days; a small amount of $Ni_{11}(TeO_3)_{10}Cl_2$ was found as the impurity phase based on XRD powder studies. Hence, single crystals of $Ni_7(TeO_3)_6Cl_2$ manually selected on the basis of their unique colors were used for IR, TGA, and magnetic measurements. The purities of the samples were confirmed by XRD powder diffraction studies. IR data for $Ni_7(TeO_3)_6Cl_2$ (KBr, cm^{-1}): 791 (s), 702 (s), 637 (w), 596 (vs), 469 (m). IR data for $Ni_{11}(TeO_3)_{10}Cl_2$ (KBr, cm^{-1}): 734 (s), 691 (vs), 624 (m), 589 (m), 482 (w), 459 (w), 431 (w).

Preparation of $Ni_5(SeO_3)_4Br_2$. Red brick-shaped single crystals of $Ni_5(SeO_3)_4Br_2$ were prepared by the solid-state reaction of a mixture containing Ni_2O_3 (0.199 g, 1.2 mmol), $NiBr_2$ (0.131 g, 0.6 mmol), and SeO_2 (0.266 g, 2.4 mmol). The reaction mixture was thoroughly ground and pressed into a pellet, which was then sealed into an evacuated quartz tube. The quartz tube was heated at 300 °C for 1 day and 670 °C for 6 days and then cooled to 310 °C at 4 °C/h before the furnace was switched off. $NiSeO_3$ (brick, yellow) was found to be the only impurity. The Ni/Se/Br molar ratio of 5.0:3.7:2.3 measured by microprobe elemental analysis is in good agreement with that determined from single-crystal X-ray structural analysis. A lot of effort was made to synthesize a single phase product for $Ni_5(SeO_3)_4Br_2$ by the solid-state reaction of a mixture containing NiO/$NiBr_2$/SeO_2 in a molar ratio of 4:1:4 at various temperatures. However, the $NiSeO_3$ impurity always exists. The highest yield of about 85% was obtained by the reaction of a mixture of Ni_2O_3/$NiBr_2$/SeO_2 in a molar ratio of 2:1:4 at 620 °C for 6 days. Hence, the samples used for its IR, TGA, and magnetic measurements are single crystals selected on the basis of their unique color. IR data for $Ni_5(SeO_3)_4Br_2$ (KBr, cm^{-1}): 841 (w), 814(m), 777 (s), 736 (vs), 715 (vs), 544 (m), 503 (m).

Single-Crystal Structure Determination. Data collections were performed on either a Rigaku Mercury CCD diffractometer (for $Ni_7(TeO_3)_6Cl_2$ and $Ni_5(SeO_3)_4Br_2$) or a Rigaku Saturn70 CCD for $Ni_{11}(TeO_3)_{10}Cl_2$) equipped with graphite-monochromated Mo Kα radiation (λ = 0.71073 Å) at 293 K. All three data sets were corrected for Lorentz and polarization factors. Absorption corrections by the multiscan method were applied for $Ni_7(TeO_3)_6Cl_2$ and $Ni_5(SeO_3)_4Br_2$ and by the numerical method for $Ni_{11}(TeO_3)_{10}Cl_2$.[14a] All three structures were solved by the direct methods and refined by full-matrix least-squares fitting on F^2 by SHELX-97.[14b] All atoms were refined with anisotropic thermal parameters. For $Ni_{11}(TeO_3)_{10}Cl_2$, Ni(6) is only 50% occupied, and three tellurite oxygen atoms are disordered and each displays two orientations (O(4) and O(4′), O(5) and O(5′), O(15) and O(15′)) with 50% occupancy each. Crystallographic data and structural refinements for the three compounds are summarized in Table 1. Important bond distances are listed in Table 2. More details of the crystallographic studies as well as atomic displacement parameters are given as Supporting Information.

Results and Discussion

Solid-state reactions of nickel(II)/(III) oxide, nickel(II) halides, and TeO_2 or SeO_2 in different molar ratios and at different temperatures yielded three new nickel tellurium(IV) and selenium(IV) oxyhalides, namely, $Ni_7(TeO_3)_6Cl_2$, $Ni_5(SeO_3)_4Br_2$, and $Ni_{11}(TeO_3)_{10}Cl_2$. All of them belong to new members in the family of nickel(II) tellurium(IV)/selenium(IV) oxyhalides with a general formula of $Ni_{n+1}(QO_3)_nX_2$ (Q = Te, X = Cl, n = 6, 10; Q = Se, X = Br, n = 4).

The structure of $Ni_7(TeO_3)_6Cl_2$ features a novel 3D network based on Ni_4ClO_3 cubane-like clusters with Te atoms

---

[12] (a) Shen, Y.-L.; Mao, J.-G.; Jiang, H.-L. *J. Solid State Chem.* **2005**, *178*, 2942. (b) Johnsson, M.; Lidin, S.; Törnroos, K. W.; Bürgi, H.-B.; Millet, P. *Angew. Chem., Int. Ed.* **2004**, *43*, 4292.

[13] Barrett, C. A.; Evans, E. B. *J. Am. Ceram. Soc.* **1964**, *47*, 533.

[14] (a) *CrystalClear*, version 1.3.5; Rigaku Corp.: The Woodlands, TX, 1999. (b) Sheldrick, G. M. *SHELXTL*, version 5.1; Bruker-AXS: Madison, WI, 1998.

Table 1. Crystal Data and Structure Refinements for $Ni_7(TeO_3)_6Cl_2$, $Ni_5(SeO_3)_4Br_2$, and $Ni_{11}(TeO_3)_{10}Cl_2$

	$Ni_7(TeO_3)_6Cl_2$	$Ni_5(SeO_3)_4Br_2$	$Ni_{11}(TeO_3)_{10}Cl_2$
empirical formula	$Cl_2Ni_7O_{18}Te_6$	$Br_2Ni_5O_{12}Se_4$	$Cl_2Ni_{11}O_{30}Te_{10}$
fw	1535.47	961.21	2472.71
space group	$R\bar{3}$ (No. 148)	$P\bar{1}$ (No. 2)	$P\bar{1}$ (No. 2)
a (Å)	11.151(4)	6.430(3)	9.281(3)
b (Å)	11.151(4)	7.632(3)	9.423(3)
c (Å)	13.450(6)	7.658(3)	10.113(3)
α (deg)	90.0	68.017(16)	100.218(1)
β (deg)	90.0	74.181(16)	99.068(4)
γ (deg)	120.0	81.465(19)	115.880(2)
V (Å^3)	1448.4(9)	334.8(3)	755.0(4)
Z	3	1	1
D_c (g cm^{-3})	5.281	4.767	5.438
μ(Mo Kα) (mm^{-1})	15.926	23.798	16.450
GOF on F^2	1.323	1.034	1.059
R1, wR2 [$I > 2\sigma(I)$][a]	0.0314, 0.0799	0.0393, 0.0940	0.0232, 0.0556
R1, wR2 (all data)[a]	0.0325, 0.0807	0.0461, 0.0975	0.0272, 0.0567

[a] $R1 = \sum||F_o| - |F_c||/\sum|F_o|$, $wR2 = \{\sum w[(F_o)^2 - (F_c)^2]^2/\sum w[(F_o)^2]^2\}^{1/2}$.

Table 2. Important Bond Lengths (Å) for $Ni_7(TeO_3)_6Cl_2$, $Ni_5(SeO_3)_4Br_2$, and $Ni_{11}(TeO_3)_{10}Cl_2$[a]

	$Ni_7(TeO_3)_6Cl_2$		
Ni(1)−O(3)#1	1.987(5)	Ni(1)−O(2)#2	2.015(4)
Ni(1)−O(2)#3	2.047(4)	Ni(1)−O(1)#4	2.076(4)
Ni(1)−O(1)	2.096(4)	Ni(1)−Cl(1)	2.487(2)
Ni(2)−O(1)#7	2.076(4)	Ni(2)−O(1)#5	2.076(4)
Ni(2)−O(1)	2.076(4)	Ni(2)−O(1)#6	2.076(4)
Ni(2)−O(1)#4	2.076(4)	Ni(2)−O(1)#2	2.076(4)
Te(1)−O(3)	1.831(5)	Te(1)−O(2)	1.878(4)
Te(1)−O(1)	1.945(4)		
	$Ni_5(SeO_3)_4Br_2$		
Ni(1)−O(6)#1	2.012(5)	Ni(1)−O(6)#2	2.026(5)
Ni(1)−O(4)	2.032(5)	Ni(1)−O(1)#3	2.112(5)
Ni(1)−O(3)#4	2.121(5)	Ni(1)−Br(1)	2.690(2)
Ni(2)−O(1)#3	2.010(5)	Ni(2)−O(1)#5	2.010(5)
Ni(2)−O(5)#6	2.043(5)	Ni(2)−O(5)	2.043(5)
Ni(2)−Br(1)	2.676(1)	Ni(2)−Br(1)#6	2.676 (1)
Ni(3)−O(4)	2.007(5)	Ni(3)−O(2)#7	2.032(5)
Ni(3)−O(2)	2.040(5)	Ni(3)−O(3)#4	2.056(5)
Ni(3)−O(5)#2	2.075(5)	Ni(3)−Br(1)#8	2.972(2)
Se(1)−O(2)	1.707(5)	Se(1)−O(1)	1.708(5)
Se(1)−O(3)	1.711(5)	Se(2)−O(6)	1.690(5)
Se(2)−O(5)	1.707(5)	Se(2)−O(4)	1.709(5)
	$Ni_{11}(TeO_3)_{10}Cl_2$		
Ni(1)−O(5′)#1	2.035(2)	Ni(1)−O(9)#1	2.046(4)
Ni(1)−O(14)#1	2.059(4)	Ni(1)−O(14)#2	2.072(4)
Ni(1)−O(3)	2.094(4)	Ni(1)−O(5)#1	2.095(2)
Ni(1)−Cl(1)	2.482(2)	Ni(2)−O(6)	1.984(4)
Ni(2)−O(1)#3	2.021(4)	Ni(2)−O(8)#1	2.054(4)
Ni(2)−O(12)#1	2.060(4)	Ni(2)−O(7)#3	2.072(4)
Ni(2)−O(1)#1	2.308(4)	Ni(3)−O(13)	2.060(4)
Ni(3)−O(7)	2.063(4)	Ni(3)−O(10)	2.064(4)
Ni(3)−O(2)#1	2.087(4)	Ni(3)−O(9)	2.094(4)
Ni(3)−O(2)	2.104(4)	Ni(4)−O(11)#1	2.029(4)
Ni(4)−O(10)	2.030(4)	Ni(4)−O(3)	2.074(4)
Ni(4)−O(5′)#1	2.083(2)	Ni(4)−O(5)#1	2.140(15)
Ni(4)−O(12)#4	2.156(4)	Ni(4)−O(12)#5	2.168(4)
Ni(5)−O(4)#1	1.910(2)	Ni(5)−O(8)	1.984(4)
Ni(5)−O(10)#1	2.075(4)	Ni(5)−O(2)	2.164(4)
Ni(5)−O(4′)#1	2.202(19)	Ni(5)−O(9)	2.254(4)
Ni(5)−O(5)	2.366(9)	Ni(6)−O(15)#6	1.951(8)
Ni(6)−O(15′)#3	2.009(8)	Ni(6)−O(11)#5	2.042(4)
Ni(6)−O(6)	2.087(5)	Ni(6)−O(7)#3	2.100(4)
Te(1)−O(3)	1.848(4)	Te(1)−O(1)	1.882(4)
Te(1)−O(2)	1.926(4)	Te(2)−O(5′)	1.817(16)
Te(2)−O(6)#8	1.842(4)	Te(2)−O(4′)#8	1.84(3)
Te(2)−O(4)#8	1.85(2)	Te(2)−O(5)	1.889(15)
Te(3)−O(8)	1.888(4)	Te(3)−O(7)	1.900(4)
Te(3)−O(9)	1.934(4)	Te(4)−O(11)#9	1.866(4)
Te(4)−O(10)#8	1.938(4)	Te(4)−O(12)	1.960(4)
Te(4)−O(13)#8	2.450(4)	Te(5)−O(15)#10	1.659(9)
Te(5)−O(15′)	1.771(8)	Te(5)−O(14)	1.851(4)
Te(5)−O(13)	1.877(4)		

[a] Symmetry transformations used to generate equivalent atoms. $Ni_7(TeO_3)_6Cl_2$: #1 $-x + 1, -y + 2, -z$; #2 $y - 1/3, -x + y + 1/3, -z + 1/3$; #3 $-y + 4/3, x - y + 5/3, z - 1/3$; #4 $-x + y, -x + 1, z$; #5 $-x + 2/3, -y + 4/3, -z + 1/3$; #6 $-y + 1, x - y + 1, z$; #7 $x - y + 2/3, x + 1/3, -z + 1/3$. $Ni_5(SeO_3)_4Br_2$: #1 $x - 1, y, z$; #2 $-x + 1, -y, -z + 1$; #3 $x, y - 1, z$; #4 $-x, -y + 1, -z + 1$; #5 $-x + 1, -y + 1, -z$; #6 $-x + 1, -y, -z$; #7 $-x + 1, -y + 1, -z + 1$; #8 $x, y, 1 + z$. $Ni_{11}(TeO_3)_{10}Cl_2$: #1 $-x + 1, -y + 1, - z + 1$; #2 $x, y, z + 1$; #3 $x + 1, y, z$; #4 $-x, -y + 1, -z + 1$; #5 $x, y - 1, z$; #6 $-x + 1, -y, -z + 1$; #7 $-x + 1, -y, -z$; #8 $x, y + 1, z$; #9 $x - 1, y, z$; #10 $x, y, z - 1$.

located at the cavities of the network (Figure 1). The asymmetric unit of $Ni_7(TeO_3)_6Cl_2$ contains a Ni(1) atom in the general position, a Ni(2) atom in a site of −3 symmetry, one tellurite group on general sites, and one Cl atom in a site of −1 symmetry. Ni(1) is octahedrally coordinated by five oxygen atoms and one chloride anion, whereas Ni(2) is octahedrally coordinated by six oxygen atoms. The Ni−Cl distances (2.487(2) Å) are significantly longer than the Ni−O bond lengths (1.987(5)−2.096(4) Å). The Te atom is in a ψ-TeO_3 trigonal pyramidal geometry with the lone pair of Te(IV) occupying the pyramidal site. Each TeO_3 group bridges with six nickel(II) ions: O(1) is monodentate, and O(2) is bidentate, whereas O(3) connects with three nickel(II) ions. Each chloride anion also bonds with three Ni(II) ions. Bond-valence calculations indicate that the nickel and tellurium atoms are 2+ and 4+, respectively. The calculated total bond valences are 1.86 (Ni(1)), 1.92 (Ni(2)), and 3.88 (Te(1)).[15]

Three $Ni(1)O_5Cl$ moities and one $Ni(2)O_6$ unit forms a Ni_4ClO_3 cubane-like cluster via O···O and O···Cl edge sharing (Figure 2a). The four nickel(II) ions within a cluster form a slightly distorted tetrahedron with Ni(1)···Ni(1) and Ni(1)···Ni(2) separations of 3.302(1) and 3.044(1) Å, respectively. Such M_4O_3Cl cluster units have been reported in a number of manganese(II) and copper(II) coordination complexes.[16] Most of the cubane clusters in the above metal complexes are isolated, but they can form a $Cu_7O_6X_2$ dimeric unit in the copper(II) complexes.[16d,16e] For nickel(II) complexes, an isolated Ni_4F_4 cubane cluster and a large number of Ni_4O_4 cubane clusters, most of them isolated, have been reported.[17] Ni_4O_4 cubane clusters were reported to be able to form super cubane clusters via corner, edge, or face sharing.[17]

It is interesting to note that each pair of cubanes in $Ni_7(TeO_3)_6Cl_2$ are also condensed into a dimeric unit by

---

(15) (a) Brown, I. D.; Altermatt, D. *Acta Crystallogr.* **1985**, *B41*, 244. (b) Brese, N. E.; O'Keeffe, M. *Acta Crystallogr.* **1991**, *B47*, 192.

(16) (a) Bashkin, J.; Chang, H.-R.; Streib, W. E.; Huffman, J. C.; Hendrickson, D. N.; Christou, G. *J. Am. Chem. Soc.* **1987**, *109*, 6502. (b) Hendrichson, D. N.; Christou, G.; Schmitt, E. A.; Libby, E.; Bashkin, J. S.; Wang, S.; Tsai, H.-L.; Vincent, J. B.; Boyd, P. D. W.; Huffman, J. C.; Folting, K.; Li, Q.; Streib, W. E. J. *Am. Chem. Soc.* **1992**, *114*, 2455. (c) Wemple, M. W.; Adams, D. M.; Folting, K.; Hendrickson, D. N.; Christou, G. *J. Am. Chem. Soc.* **1995**, *117*, 7275. (d) Liu, X.; McAllister, J. A.; de Miranda, M. P.; Mclnnes, E. J. L.; Kilner, C. A.; Halcrow, M. A. *Chem.*−*Eur. J.* **2004**, *10*, 1827. (e) Liu, X.; McAllister, J. A.; de Miranda, M. P.; Whitaker, B. J.; Kilner, C. A.; Thornton-Pett, M.; Halcrow, M. A. *Angew. Chem., Int. Ed.* **2002**, *41*, 756.

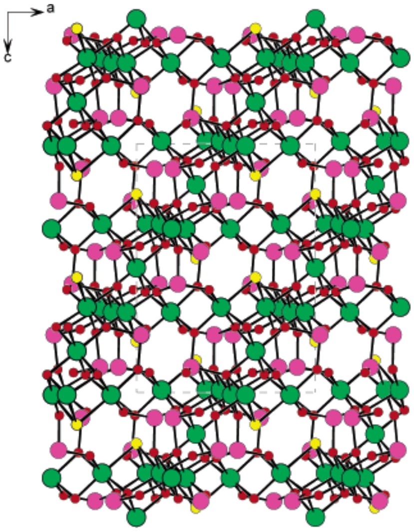

Figure 1. View of the structure of $Ni_7(TeO_3)_6Cl_2$ along the *b* axis. Ni, Te, O, and Cl atoms are represented by green, purple, red, and yellow circles, respectively.

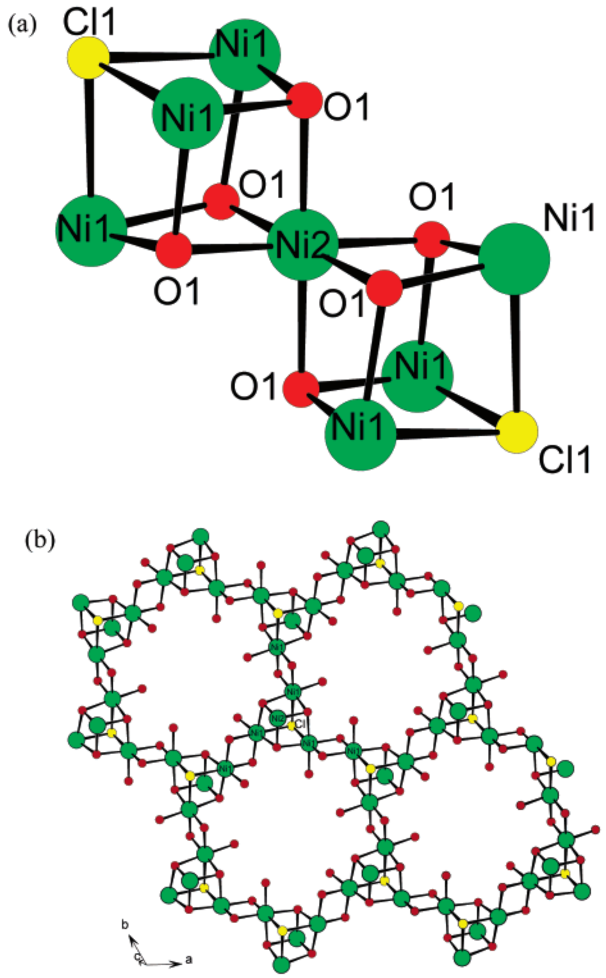

Figure 2. Two Ni_4O_3Cl cubane cluster units sharing a Ni^{2+} ion in $Ni_7(TeO_3)_6Cl_2$ (a). A 2D layer normal to the *c* axis based on Ni_4O_3Cl cubane cluster units bridged by a pair of oxygen atoms in $Ni_7(TeO_3)_6Cl_2$ (b). Ni, O, and Cl atoms are represented by green, red, and yellow circles, respectively.

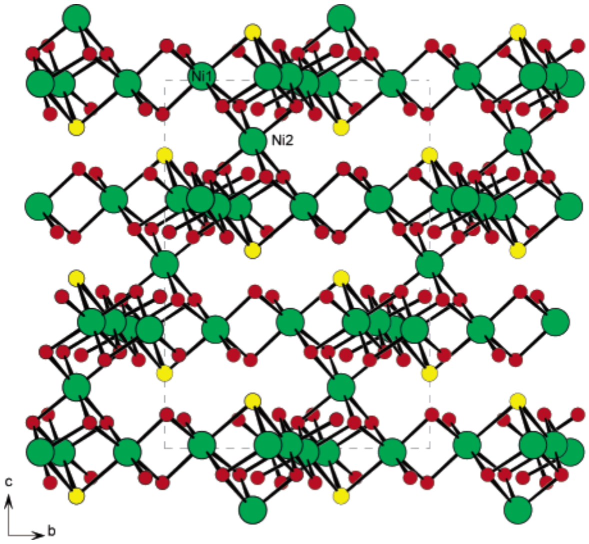

Figure 3. 3D network of nickel(II) oxychloride in $Ni_7(TeO_3)_6Cl_2$. Ni, O, and Cl atoms are represented by green, red, and yellow circles, respectively.

sharing a Ni(2) atom (Figure 2a). Along the *ab* plane, the Ni_4ClO_3 cubanes are interconnected via O(2)···O(2) edge sharing into a novel 2D cluster layer, forming 12-member polyhedral rings (Figure 2b). Each ring is composed of six Ni_4ClO_3 cubanes; hence, such cubane cluster layers are to some extent similar to those of graphite. The intercluster Ni(1)···Ni(1) distance of 2.877(1) Å is the shortest among all Ni···Ni separations. The adjacent layer can be viewed as generated by moving the former layer by $-{}^1/_3a + {}^1/_3b + {}^1/_3c$. Neighboring layers are interconnected by sharing Ni(2) atoms into a 3D network with small long-narrow-shaped tunnels along the *a* axis (Figure 3). To the best of our knowledge, this is the first example of a 3D network based on cubane clusters. The Te atoms are located at the above tunnels and connected to the cubanes via Te−O bonds. It should be pointed out that such stacking of the cluster layers eliminates the large tunnels along *c* axis created by 12-member rings.

$Ni_5(SeO_3)_4Br_2$ features a 3D network different from that of $Ni_5(SeO_3)_4Cl_2$ previously reported by us.[12a] Its 3D structure can be viewed as nickel(II) oxy-bromide layers being bridged by Se(IV) and additional Ni(II) ions (Figure 4a). The asymmetric unit of $Ni_5(SeO_3)_4Br_2$ contains three unique Ni(II) ions, two selenite anions, and a bromide anion. Ni(1) and Ni(3) are in the general position and Ni(2) occupies a site with -1 symmetry, which is different from that of $Ni_5(SeO_3)_4Cl_2$ which contains five unique Ni(II) ions, four selenite anions and two chloride anions, all of which are in the general sites.[12a] Both Ni(1) and Ni(3) are octahedrally coordinated by five selenite oxygen atoms and a bromide anion, whereas Ni(2) is in a distorted octahedral environment composed of two bromide anions and four oxygen atoms. The Ni−Br distances (2.676(1)−2.972(2) Å) are significantly longer than the Ni−O distances (2.007(5)−2.121(5) Å). Each

---

(17) (a) Schroter, M.; Lork, E.; News, R. *Z. Anorg. Allg. Chem.* **2005**, *631*, 1609. (b) Shaw, R.; Tidmarsh, I. S.; Laye, R. H.; Breeze, B.; Helliwell, M.; Brechin, E. K.; Heath, S. L.; Murrie, M.; Ochsenbein, S.; Güdel, H.-U.; McInnes, E. J. L. *Chem. Commun.* **2004**, 1418. (c) Murrie, M.; Biner, D.; Stoeckli-Evans, H.; Güdel, H.-U. *Chem. Commun.* **2003**, 230. (d) Cromie, S.; F. Launay, F.; McKee, V.; *Chem. Commun.* **2001**, 1918. (e) Brechin, E. K.; Clegg, W.; Murrie, M.; Parsons, S.; Teat, S. J.; Winpenny, R. E. P. *J. Am. Chem. Soc.* **1998**, *120*, 7366.

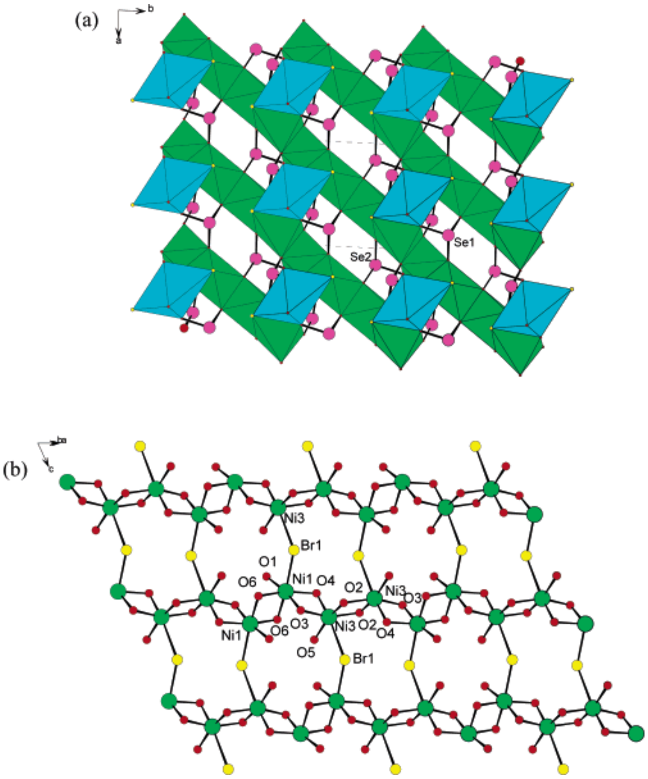

Figure 4. View of the structure of $Ni_5(SeO_3)_4Br_2$ down the *c*-axis (a) and the 2D nickel(II) oxybromide layer in $Ni_5(SeO_3)_4Br_2$ (b). $Ni(1)O_5Br$ and $Ni(3)O_5Br$ octahedra are shaded in green and $Ni(2)O_4Br_2$ octahedra are shaded in cyan.

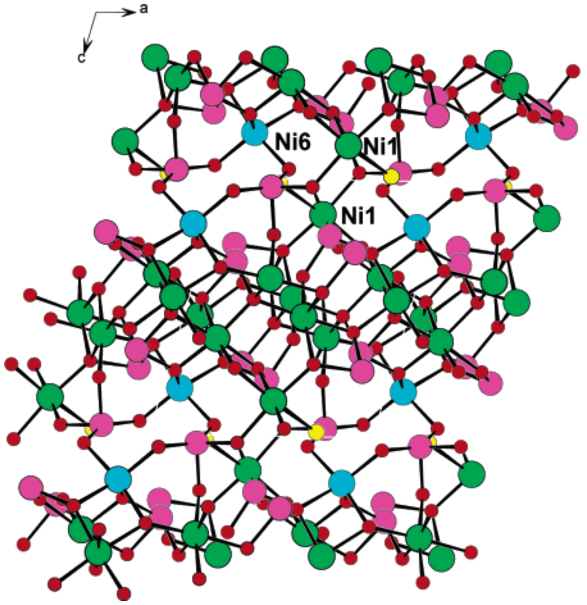

Figure 5. View of the structure of $Ni_{11}(TeO_3)_{10}Cl_2$ down the *b* axis. Ni(6) atoms are drawn as cyan circles. The other Ni atoms are represented by green circles. Te, O, and Cl atoms are shown as pink, red, and yellow circles, respectively.

bromide anion is tridentate as the chloride anion in $Ni_7(TeO_3)_6Cl_2$. Bond-valence calculations indicate nickel and selenium atoms are 2+ and 4+, respectively. The calculated total bond valences are 1.92 (Ni(1)), 1.96 (Ni(2)), 1.87 (Ni(3)), 3.96 (Se(1)), and 4.03 (Se(2)).[15]

$Ni(1)O_5Br$ and $Ni(3)O_5Br$ octahedra are interconnected via edge-sharing (O···O) into a 1D chain and neighboring chains are further interconnected via corner-sharing (Br) into a 2D architecture (Figure 4b). The Ni···Ni distances between Ni(II) ions bridged by a pair of oxygen atoms fall in the range of 3.034(1)−3.243(1) Å, whereas the Ni···Ni separation between two nickel(II) ions bridged by a pair of bromide anions is 5.333(1) Å. The above 2D nickel oxybromide layers are further interconnected by Ni(2) and Se(IV) atoms into a condensed 3D network (Figure 4a). Ni(2) atoms are edge sharing (Br−O) with Ni(1) and Ni(3) with Ni···Ni separations of 3.289(1) and 3.415(1) Å. Such a 3D network can also be viewed as a pillared layered structure in which Ni(2) and selenite groups act as pillars (Figure 4a). This type of structure is different from that of $Ni_5(SeO_3)_4Cl_2$ whose 3D network can also be considered to be formed by the interconnection of nickel(II) octahedra via corner, edge, and face sharing with Se^{4+} ions capping the cavities.[12a]

The structure of $Ni_{11}(TeO_3)_{10}Cl_2$ features a very complicated 3D network (Figure 5). There are six unique nickel(II) ions, five tellurite groups and one chloride anion in the asymmetric unit of $Ni_{11}(TeO_3)_{10}Cl_2$: all of them occupy the general sites. The Ni(6) site is only 50% occupied, and the three tellurite oxygens (O(4), O(5) and O(15)) are disordered, each displaying two orientations. Partially occupation for the nickel and halide sites have been also reported in a number of nonstoichiometric nickel Te(IV) oxyhalides.[12b] All of these compounds can be considered to be derivatives of the $Ni_{n+1}(QO_3)_nX_2$ family where $n > 10$. It is obvious that disorder or nonstoichiometry is very likely for those members with higher n values.

The coordination geometry around the Ni(1) atom is a distorted octahedron composed of one chloride and five oxygen atoms. Ni(2), Ni(3), and Ni(4) are octahedrally coordinated by six tellurite oxygen atoms, whereas Ni(5) and Ni(6) are in the square pyramidal geometry composed of five oxygen atoms (two oxygen atoms of the $Ni(6)O_5$ polyhedron are only 50% occupied). The Ni−Cl distance of 2.482(2) Å is significantly longer than those of the Ni−O bonds (1.910(2)−2.366(9) Å). All of Te atoms are in a ψ-TeO_3 trigonal pyramidal geometry with the lone pair of Te(IV) occupying the pyramidal site. One oxygen atom of the $Te(5)O_3$ group is distorted over two orientations as mentioned earlier. Te−O distances are in the range of 1.659(9)−1.960(4) Å. It should be mentioned that Te(4) also forms a very weak Te−O bond with a greatly elongated distance (Te(4)−O(13) 2.445(5) Å). Unlike those in $Ni_7(TeO_3)_6Cl_2$ and $Ni_5(SeO_3)_4Br_2$, the halide anions in $Ni_{11}(TeO_3)_{10}Cl_2$ are unidentate.

The interconnection of above NiO_5Cl, NiO_6, and NiO_5 polyhedra via corner and edge sharing leads to a complex 3D network of nickel oxychloride (Figure 6a). The Te(IV) atoms are located at the voids of the network and also connect with the framework through Ni−O−Te bridges (Figure 5). The Ni···Ni separations between two edge-sharing nickel(II) coordination octahedra are in the range of 2.983(1)−3.305(1) Å, and those between corner-sharing ones range from 3.377(1) to 3.495(1) Å. The 3D nickel oxychloride network can also be considered as a pillared layered

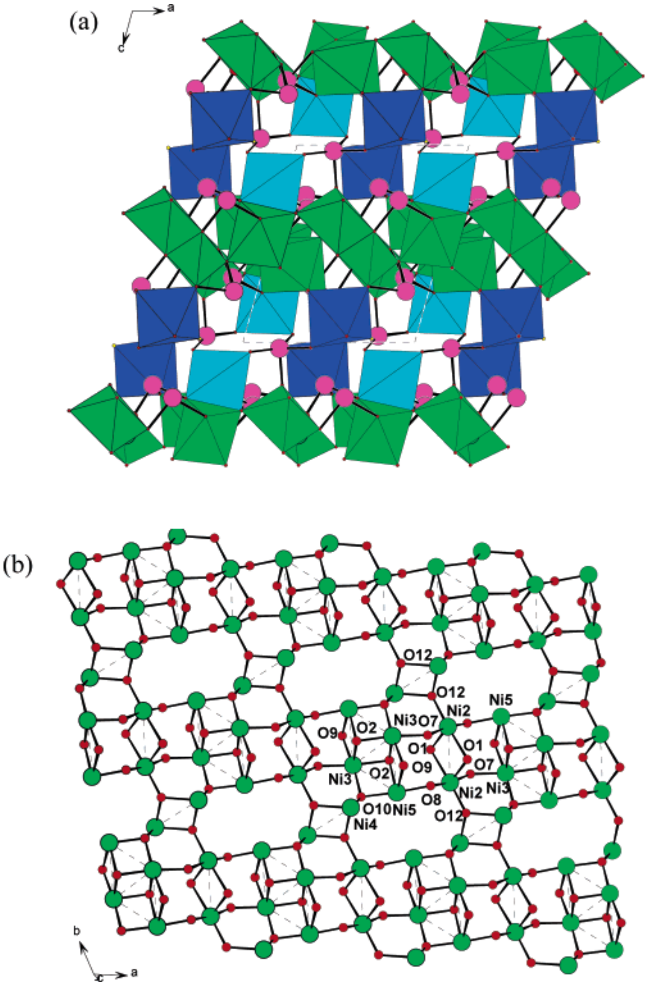

Figure 6. View of the 3D network structure of nickel(II) oxychloride in $Ni_{11}(TeO_3)_{10}Cl_2$ down the *b* axis (a) and a (002) nickel(II) oxide layer composed of Ni(2), Ni(3), Ni(4), and Ni(5) atoms (b). The Ni(2), Ni(3), Ni(4), and Ni(5) polyhedra are shaded in green, whereas those of Ni(1) and Ni(6) are shaded in blue and cyan, respectively.

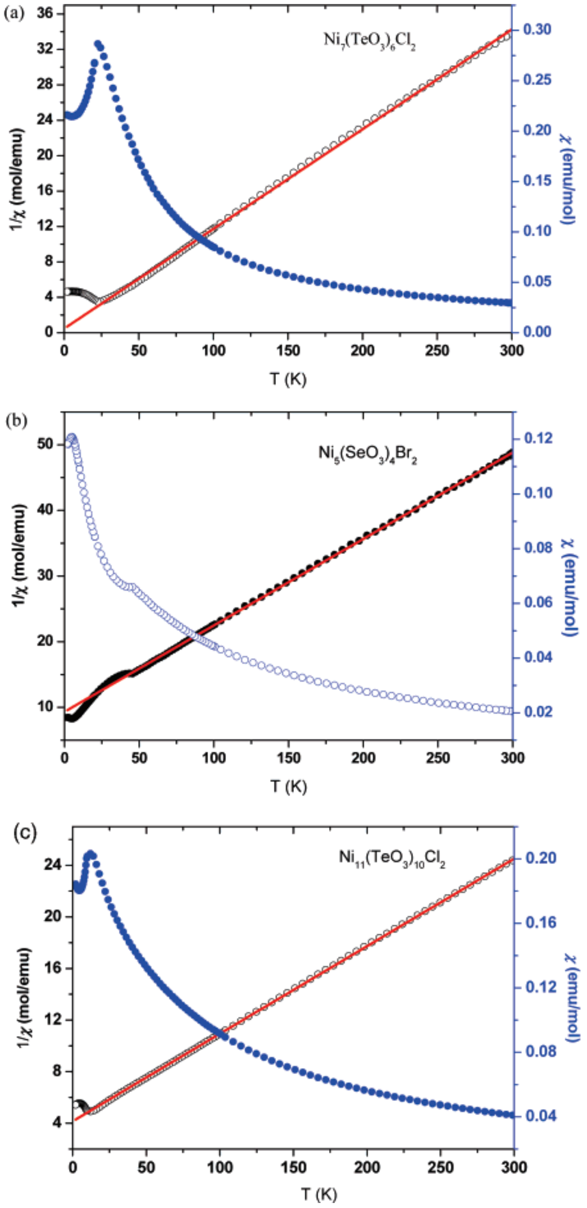

Figure 7. χ vs T and $1/\chi$ vs T plots for $Ni_7(TeO_3)_6Cl_2$ (a), $Ni_5(SeO_3)_4Br_2$ (b), and $Ni_{11}(TeO_3)_{10}Cl_2$ (c). The red line represents the linear fit of data according to the Curie−Weiss Law.

architecture based on the nickel oxide layers composed of Ni(2), Ni(3), Ni(4), and Ni(5) (Figure 6b). $Ni(6)O_5$ polyhedra are attached on both sides of the above nickel oxide layer; each pair of $Ni(1)O_5Cl$ octahedra form a dimeric unit via edge sharing (O(14)−O(14)), and they act as pillars between the two neighboring nickel oxide layers.

Magnetic Properties. $Ni_7(TeO_3)_6Cl_2$ obeys the Curie−Weiss Law in the temperature range of 25−300 K; below 25 K, a large deviation was observed (Figure 7a). The existence of a maximum of molar susceptibility at 22.5 K is indicative of long-range magnetic ordering at low temperature. At 300 K, the effective magnetic moment (μ_{eff}) is 8.40 μ_B, which corresponds to seven isolated Ni^{2+} ($S = 1$, $g = 2.24$) ions. It decreases continuously upon cooling and reaches 1.85 μ_B at 2.0 K. A linear fit of the magnetic data in the range of 100−300 K gave a Weiss constant of −10.4 (2) K, indicating significant antiferromagnetic interactions between magnetic centers. As mentioned earlier, the Ni···Ni separations between Ni(II) ions within a cubane-like cluster unit are 3.302(1) and 3.044(1) Å, respectively. The intercluster Ni(1)···Ni(1) distance is 2.877(1) Å. ZFC and FC measurements indicate that the maximum of susceptibility remains almost unchanged below T_c (22.5 K) and that the molar susceptibility increases slightly with increasing magnetic field (see Supporting Information). $Ni_5(SeO_3)_4Br_2$ obeys the Curie−Weiss Law in the temperature range of 50−300K; below 50 K a significant deviation was observed (Figure 7b). At 300 K, the effective magnetic moment (μ_{eff}) is 7.0 μ_B, which corresponds to five isolated Ni^{2+} ($S = 1$, $g = 2.21$) ions. It decreases continuously upon cooling and reaches 1.37 μ_B at 2.0 K. The linear fit of the magnetic data in the range of 100−300 K gave a Weiss constant of −74.4 (2) K, indicating very strong antiferromagnetic interactions between Ni^{2+} ions. It is expected that the magnetic interactions should be dominated by the magnetic interactions between Ni(II) polyhedra sharing O−O or O−Br edges (Ni···Ni = 3.034(1)−3.415(1) Å). $Ni_{11}(TeO_3)_{10}Cl_2$ obeys the Curie−Weiss Law in the temperature range of 12−300 K; below 12 K a significant deviation was observed (Figure 7c). The existence

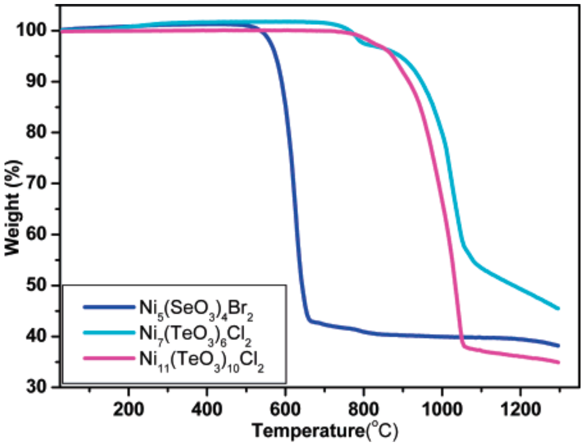

Figure 8. TGA curves for $Ni_7(TeO_3)_6Cl_2$, $Ni_5(SeO_3)_4Br_2$, and $Ni_{11}(TeO_3)_{10}Cl_2$.

of a maximum of molar susceptibility at 12.0 K is indicative of long-range magnetic ordering at low temperature. At 300 K, the effective magnetic moment (μ_{eff}) is 9.9 μ_B, which corresponds to eleven isolated Ni^{2+} ($S = 1$, $g = 2.11$) ions. It decreases continuously upon cooling and reaches 1.73 μ_B at 2.0 K. The linear fit of the magnetic data in the range of 100−300 K gave Weiss constant of −63.1 (2) K, indicating very strong antiferromagnetic interactions between Ni^{2+} ions. It is expected that the magnetic interactions should be dominated by the magnetic interactions between edge- or corner-sharing Ni(II) polyhedra (Ni···Ni = 2.983(1)−3.495(1) Å).

TGA Analysis. TGA analyses under an oxygen atmosphere indicate that $Ni_7(TeO_3)_6Cl_2$, $Ni_5(SeO_3)_4Br_2$, and $Ni_{11}(TeO_3)_{10}Cl_2$ are stable up to 700, 500, and 750 °C, respectively (Figure 8). Then, all of them exhibit one main step of weight loss (in the temperature ranges of 700−1100, 500−750, and 800−1050 °C for $Ni_7(TeO_3)_6Cl_2$, $Ni_5(SeO_3)_4Br_2$, and $Ni_{11}(TeO_3)_{10}Cl_2$, respectively), which corresponds to the release of QO_2 and halogen. The final residues are found to be mainly NiO on the basis of XRD powder studies. The observed total weight losses at 1300 °C are 61.3 and 66.0% for $Ni_5(SeO_3)_4Br_2$ and $Ni_{11}(TeO_3)_{10}Cl_2$, respectively. These values are very close to the calculated ones (61.1 and 66.8%, respectively). For $Ni_7(TeO_3)_6Cl_2$, the observed total weight loss of 56.2% is significantly smaller than the calculated value of 65.9%; hence, decomposition is incomplete at 1300 °C, as also indicated by the slope of the TGA curves. $Ni_7(TeO_3)_6Cl_2$ is thermally more stable than $Ni_5(SeO_3)_4Br_2$, which may be the result of the Ni−Br bond being weaker than the Ni−Cl bond. The higher thermal stability of $Ni_7(TeO_3)_6Cl_2$ than that of $Ni_{11}(TeO_3)_{10}Cl_2$ could be attributed to the fact that the chloride ion bridges with three nickel(II) ions in $Ni_7(TeO_3)_6Cl_2$ whereas it forms one Ni−Cl bond in $Ni_{11}(TeO_3)_{10}Cl_2$.

It is interesting to compare the structures and physical properties of compounds in this family. $Ni_5(TeO_3)_4X_2$ (X= Cl, Br, I) are isostructural and feature a layered structure built up of corner-connected $[Ni_5O_{17}X_2]$ entities. They are new compounds having a 2D $S = 1$ quantum spin system with antiferromagnetic superexchange interaction. The transition temperature increases with the interlayer distances: 23, 28, and 30 K for X = Cl, Br, and I, respectively.[9] On the other hand, the corresponding selenite compounds, $Ni_5(SeO_3)_4X_2$ (X= Cl, Br), form two types of 3D networks. $Ni_5(SeO_3)_4Br_2$ is pillar layered, and the packing of $Ni_5(SeO_3)_4Cl_2$ is more condensed with shorter Ni···Ni distances. Both compounds exhibit strong antiferromagnetic interactions between nickel(II) ions with Weiss constants of −143(2) and −74.4 (2) K for X = Cl and Br, respectively.[12a] The structure of $Ni_7(TeO_3)_6Cl_2$ features a novel 3D cluster network based on Ni_4ClO_3 cubane-like clusters. The structure of $Ni_{11}(TeO_3)_{10}Cl_2$ features a condensed 3D network based on NiO_5Cl, NiO_6, and NiO_5 polyhedra interconnected via corner and edge sharing, as well as with O−Te−O bridges. Several tellurite oxygen atoms are disordered. The three nonstoichiometric compounds, $[Ni_{30}Te_{32}O_{90}Br_{2.64}][Ni_{3.39}Br_{12.14}]$, $[Ni_{30}Te_{32}O_{90}Cl_{2.69}][Ni_{3.10}Cl_{11.52}]$, and $[Ni_{30}Te_{32}O_{90}Cl_{2.67}][Ni_{4.48}Cl_{15.78}]$ are formed at relatively lower temperatures (above 800 K). All three compounds contain covalently bonded, cationic entities of approximate composition $[Ni_{30}Te_{32}O_{90}X_3]^{5+}$ (X = Br, Cl), which form an infinite porous network enclosing large cavities that contain different guests of anionic clusters.[12b]

Conclusion

In summary, we have prepared three new compounds in the family of $Ni_{n+1}(QO_3)_nX_2$ (Q = Te, Se; X = halide). Their structures are closely related to the n value, as well as to the Q and X elements. When n is small, the structures are ordered, and nonstoichiometric compounds will be isolated if n is larger (i.e., $n > 10$). The structures of selenite compounds are usually different from those of the corresponding tellurite ones. It is very interesting that the structure of $Ni_7(TeO_3)_6Cl_2$ features a novel 3D cluster network based on Ni_4ClO_3 cubane-like clusters. Such an extended open framework based on cubane clusters provides an important addition to the family of cubane compounds. Future efforts will be devoted to the exploration of other missing members in this family.

Acknowledgment. This work was supported by National Natural Science Foundation of China (No. 20573113 and 20521101) and NSF of Fujian Province (No. E0420003).

Supporting Information Available: X-ray crystallographic files in CIF format and simulated and experimental XRD powder patterns for $Ni_7(TeO_3)_6Cl_2$, $Ni_5(SeO_3)_4Br_2$, $Ni_{11}(TeO_3)_{10}Cl_2$, and NiO. This material is available free of charge via the Internet at http://pubs.acs.org.

IC060356X